NATIONAL ADVISORY COMMITTEE FOR AERONAUTICS

TECHNICAL NOTE

No. 1061

WIND-TUNNEL INVESTIGATION OF EFFECT OF WING LOCATION,

PCWER, AND FLAP DEFLECTICN ON EFFECTIVE DIHEDRAL

CF A TYPICAL SINGLE-ENGINE FIGHTER-AIRPLANE MODEL

WITH TAIL REMOVED

By Warren A. Tucker

Langley Memorial Aeronautical Laboratory
Langley Field, Va.

Washington
May 1946

NATIONAL ADVISORY COMMITTEE FOR AERONAUTICS

TECHNICAL NOTE No. 1061

WIND-TUNNEL INVESTIGATION OF EFFECT OF WING LOCATION,

POWER, AND FLAP DEFLECTION ON EFFECTIVE DIHEDRAL

OF A TYPICAL SINGLE-ENGINE FIGHTER-AIRPLANE MODEL

WITH TAIL REMOVED

By Warren A. Tucker

SUMMARY

An investigation has been made of the effect of
wing location, power, and flap deflection on the effective
dihedral of a typical single-engine fighter-airplane model.
The model, which was tested in the Langley 7- by 10-foot
tunnel, had provisions for placing the wing in either
one of two vertical locations. The wing was fitted
alternatively with a full-span single slotted flap and
with a full-span double slotted flap. The vertical and
horizontal tails were removed for all tests.

The results are presented as curves of lateral-
stability derivatives against lift coefficient. The
observed effects are explained qualitatively. In addition
to showing the usual loss in effective dihedral caused
by changing from a high-wing to a low-wing design, the
results indicated that this loss is increased by the
application of power. The adverse effect of power increased
with lift coefficient. The effect of flap deflection,
which was unfavorable for all cases, appeared to be
slightly greater for the low-wing model.

INTRODUCTION

The problem of achieving sufficient effective dihedral
for satisfactory handling qualities at low speeds and
high thrust coefficients is becoming increasingly
important, particularly with the advent of the high-
powered low-wing fighter airplane. Some theoretical and

experimental work has been done on the effect of wing
plan form and geometric dihedral on the effective dihedral
of an isolated wing (references 1 and 2). Other experi-
mental investigations of complete models of specific
airplanes and of generalized models (references 3
to 7) have been made to determine the effect of
wing plan form and wing location, and some theoretical
work has been done on the effect of wing location (ref-
erence 8). There seems, however, to be little correlated
information available regarding the mutual effects of
power, flap deflection, and wing location.

A comprehensive investigation of the effects of wing
location, power, and flap deflection on the static
stability of a model of a single-engine fighter airplane
is being conducted in the Langley 7- by 10-foot tunnel.
The investigation includes longitudinal-stability and
lateral-stability tests of the model as a high-wing and
as a low-wing airplane. The tests have been made without
flaps, with a full-span slotted flap having a chord
25 percent of the wing chord (0.25c), and with a 0.40c
full-span double slotted flap. All tests have been made
both with the propeller windmilling and with power on.
Data on the effect of wing location, power, and flap
deflection on effective dihedral with the tail removed
have been obtained from the tests and are presented
herein. Since the scope of the investigation was some-
what limited, particularly in the range of power, the
conclusions are not very general.

APPARATUS AND MODEL

The tests were made in the Langley 7- by 10-foot tunnel,
which is described in references 9 and 10. The basic
model was a modified $\frac{1}{5}$-scale model of the Curtiss P-36A
airplane (fig. 1). The vertical and horizontal tails
were removed for all tests. The landing gear was
retracted for all tests, since the aerodynamic effect of
landing gears on stability is usually small.

The wing without flaps corresponded to the P-36A wing.
The quarter-chord line of the wing was swept forward 2.6°.
The 0.40c double slotted flap, which covered 93 percent
span, was designed by use of the data of reference 11.
The front part of the flap was deflected 30° with

respect to the flap-retracted position; the rear part of
the flap was deflected 30° with respect to the front
part. The rear part was used as a 0.25c single slotted
flap by keeping the two parts of the flap in the same
position relative to each other but moving the whole
flap so that the front part was in the retracted position.
The front part of the flap was then faired to the air-
foil contour with modeling clay for tests of the wing
with a single slotted flap. The details of the flap are
shown in figure 2.

The model had a three-blade right-hand metal propeller.
The propeller was driven by a 56-horsepower water-cooled
induction motor mounted in the fuselage nose. The motor
speed was measured by use of a cathode-ray oscillograph,
which indicated the output of a small alternator connected
to the shaft of the motor. The time base for the
oscillograph pattern was controlled by an audio oscillator
of the electrically driven tuning-fork type, the
frequency of which was known within ± 0.1 percent. The
propeller blade angle was set at 25° at the 0.75-radius
station for all the tests. The side-force factor of the
propeller (see reference 12) was 70.2.

TESTS AND RESULTS

Test conditions.- All tests, except the power-on tests
of the model with the double slotted flap, were made at a
dynamic pressure of 16.37 pounds per square foot, which
corresponds to a velocity of 80 miles per hour at standard
sea-level conditions. In order to obtain the required
thrust coefficients from the model motor, the power-on
tests of the model with the double slotted flap were
made at a dynamic pressure of 12.53 pounds per square
foot, which corresponds to a velocity of 70 miles per
hour at standard sea-level conditions. The corresponding
test Reynolds numbers for these velocities were
about 1,000,000 and 875,000, respectively, based on the
model wing mean aerodynamic chord of 16.32 inches. The
corresponding effective Reynolds numbers, based on the
tunnel turbulence factor of 1.6, were about 1,600,000
and 1,400,000, respectively.

Coefficients and symbols.- The results of the tests
are presented in the form of standard NACA nondimensional
coefficients of forces and moments. Rolling-moment and

yawing-moment coefficients are given about the center-of-gravity location shown in figure 1 (26.7 percent M.A.C.). The data are referred to a system of axes in which the Z-axis is in the plane of symmetry and perpendicular to the relative wind, the X-axis is in the plane of symmetry and perpendicular to the Z-axis, and the Y-axis is perpendicular to the plane of symmetry. The axis system is shown in figure 3.

The coefficients and symbols used herein are defined as follows:

C_L lift coefficient (Z/qS)

C_{D_R} resultant-drag coefficient (X/qS)

C_Y lateral-force coefficient (Y/qS)

C_l rolling-moment coefficient (L/qSb)

C_m pitching-moment coefficient $(M/qS\bar{c})$

C_n yawing-moment coefficient (N/qSb)

T_c' effective thrust coefficient based on wing area
         (T_e/qS)

T_c effective thrust coefficient based on propeller
         disk area $(T_e/\rho V^2 D^2)$

where

Z   lift

X   resultant drag

Y   lateral force

L   rolling moment

M   pitching moment

N   yawing moment

T_e effective thrust, pounds

q   dynamic pressure, pounds per square foot $\left(\frac{1}{2}\rho V^2\right)$

D   model propeller diameter (2.0 ft)

S   model wing area (9.44 sq ft)

b   model wing span (7.45 ft)

c   model wing chord

$\bar{c}$ model wing mean aerodynamic chord (16.32 in.)

and

ρ mass density of air, slugs per cubic foot

V   velocity, feet per second

R   propeller radius

n   propeller speed, revolutions per second

β model propeller blade angle at 0.75R

η propeller efficiency

α_T angle of attack of thrust line, degrees

ψ angle of yaw, degrees

δ_f or δ_{f_2} deflection of rear part of flap with respect
        to front part, degrees

δ_{f_1} deflection of front part of flap with respect to
        flap-retracted position, degrees

The subscript ψ denotes the partial derivative of a
coefficient with respect to the angle of yaw; for example,

$$C_{l_\psi} = \frac{\partial C_l}{\partial \psi}$$

Test procedure.- Propeller calibrations were made
by measuring the resultant drag of the model at zero
angle of attack, with flaps neutral, and with tail removed
for a range of propeller speed. The effective thrust
coefficient based on wing area was then computed from
the relation

$$T_c' = C_D - C_{D_R}$$

where C_D is the drag coefficient of the model with the propeller removed. Motor torque, from which the propeller efficiency was computed, was measured with a built-in strain-gage torque dynamometer. The propeller calibration, which was made for only the low-wing model, is shown in figure 4; it is thought that the calibration for the high-wing model would be the same.

The variations of the effective thrust coefficient based on wing area T_c' and the effective thrust coefficient based on propeller disk area T_c with the lift coefficient C_L used for the tests are given in figure 5. A straight-line variation was used because this variation is a close approximation to the variation for airplanes with constant-speed propellers operating at constant power. The use of a straight-line variation is an assumption that $\eta / \sqrt{C_L}$ is a constant; for this case, the value of $\eta / \sqrt{C_L}$ was about 0.98. Although this assumption requires propeller efficiencies that would never be reached at low lift coefficients on an actual airplane, the error in T_c' is small because the values of T_c' are small. The approximate amount of airplane engine horsepower represented is given in figure 6 for various assumed wing loadings and model scales. The horsepower represented is proportional to the wing loading raised to the three-halves power and to the reciprocal of the square of the model scale.

Tests were made through the range of angle of attack and at angles of yaw of 5° and -5° to determine the slopes $C_{l\psi}$, $C_{n\psi}$, and $C_{Y\psi}$ for various power conditions and model configurations. A linear variation between $\psi = -5°$ and $\psi = 5°$ was assumed for the corresponding coefficients C_l, C_n, and C_Y. The results therefore are not necessarily applicable at large angles of yaw.

Corrections.- All data for power-on tests have been corrected for tares caused by the model support strut. The data for windmilling tests have not been corrected for these tares because of the limited time available for the tests; it is believed that the tares for the windmilling condition would be relatively small.

The angles of attack and the drag coefficients have been corrected for tunnel-wall effects. The corrections were computed as follows:

$$\Delta \alpha_T = 57.3 \delta_w \frac{S}{C} C_L \qquad (\text{deg})$$

$$\Delta C_D = \delta_w \frac{S}{C} C_L{}^2$$

where

δ_w jet-boundary correction factor at wing (0.113)

S   model wing area (9.44 sq ft)

C   tunnel cross-sectional area (69.59 sq ft)

The corrections were added to the test data.

    <u>Results</u>.- The parameters C_{l_ψ}, C_{n_ψ}, and C_{Y_ψ} obtained at angles of yaw of $\pm 5°$ are given in figure 7. The curves of C_{n_ψ} and C_{Y_ψ} are included for completeness in these standard lateral-stability plots. Figures 8, 9, and 10, showing the effects on C_{l_ψ} of wing location, power, and flap deflection, respectively, were obtained by taking the increments between the appropriate curves of figure 7. Figure 11 shows the aerodynamic characteristics in pitch of the model at zero yaw. The effect of power on the lift coefficient, presented in figure 12, was obtained by taking the increment between the appropriate curves of figure 11.

<div align="center">DISCUSSION</div>

    In the following discussion, the observed effects are noted and some attempt is made to explain them qualitatively. A quantitative explanation seems impossible at the present stage of knowledge, because of the absence of any adequate theory covering the complex flows involved.

Effect of wing location.- The low-wing model was
tested with a geometric dihedral angle of 6°, measured
to the chord plane. When the wing was shifted to the
high location, an estimate was made from reference 3
of the amount the geometric dihedral angle would have
to be decreased in order to give the same effective
dihedral for the high-wing and the low-wing models with
flaps retracted and propeller windmilling. The estimated
necessary change in geometric dihedral angle
(about $4\frac{1}{2}^\circ$) caused the upper surface of the wing in the
high location to be very nearly straight; for ease of
construction, therefore, the upper surface was actually
made straight. The dihedral angle of the chord plane
was then 1.9°. The curve of figure 8 for the model with
propeller windmilling and flaps retracted shows that
the aim of achieving no change in effective dihedral
between the low-wing and the high-wing configurations
was very nearly realized. The curve shows that the
low-wing model has about 1° effective dihedral less than
the high-wing model over most of the lift-coefficient
range (1° of effective dihedral corresponds
to $C_{l_\psi} = 0.0002$). The effect of power with flaps
retracted was to increase this difference in effective
dihedral between the high-wing and low-wing configurations.
The reason for this effect is discussed more fully in
the section on the effect of power.

The decrease in effective dihedral caused by
lowering the wing can be explained by considering the
flow that occurs over and under the fuselage when the
model is yawed. The type of flow is illustrated in
figure 13. This transverse flow increases the angle of
attack near the fuselage of the leading wing in the
high location and decreases the angle of attack of the
leading wing in the low location. These changes in
angle of attack result in a favorable rolling moment
for the high-wing model and an unfavorable rolling
moment for the low-wing model. This explanation shows
why, in general, a high-wing airplane will exhibit
greater effective dihedral than a corresponding low-
wing airplane. Similar reasoning has been used in
reference 8 to obtain a quantitative check between
theoretical and experimental results. The explanation
has sometimes been advanced that, when the model is yawed,
a region of increased pressure is built up on the
upwind side of the fuselage and a region of decreased

pressure is built up on the downwind side. This
difference in pressure has been thought to give a
favorable dihedral effect if the wing is high or an
unfavorable effect if the wing is low. This pressure
difference occurs, however, only when the cross-sectional
area of the fuselage is increasing with distance backward
along the fuselage - near the nose, for example. (A
smaller opposite pressure difference will occur near
the tail.) Since for most airplanes the wing is located
in a region where the cross-sectional fuselage area is
not changing greatly with distance along the fuselage
and since experimental results may be checked quantitatively
by considering angle-of-attack changes, it would seem
that this explanation is not usually applicable.

With power on, the adverse effect of lowering the
wing appears to be increased for all flap positions (fig. 8).
A particularly large power effect is observed for the
model with the double slotted flap. It should be noted
that the curve for the model with double slotted flaps
and propeller windmilling is not consistent with the
other curves. This curve was derived from figure 7(c),
in which the curve for the low-wing model in the
windmilling condition is thought to be unreliable,
perhaps because of a partial stall.

The foregoing discussion of the effects of wing
location can be summarized as follows:

(1) Changing the wing from the high to the low
location results in a decrease in effective dihedral.

(2) The difference in effective dihedral for the
high-wing and the low-wing models is increased by the
application of power.

Effect of power.- The effect of power (fig. 9)
seems to be adverse for most cases. The effect is
greater for the low-wing than for the high-wing model,
and this difference in effect seems to increase with
lift coefficient. An exception is noted in the curves
for the double slotted flap. These curves, however,
were derived from figure 7(c), in which the curve for
the low-wing model in the windmilling condition is
thought to be unreliable.

A possible explanation of the greater adverse effect of power on the low-wing model is given here. The slipstream affects the dihedral effect in two ways:

(1) The increased dynamic pressure in the slipstream results in an increased lift over the part of the wing immersed in the slipstream. When the model is yawed, the center line of the slipstream tends to pass over the trailing wing. The center of pressure of the added lift due to the slipstream thus lies somewhere on the trailing wing. The resulting rolling moment is therefore unfavorable.

(2) The increased dynamic pressure over the fuselage intensifies the effect of wing-fuselage interference which, as has been seen, is in general favorable for the high-wing and unfavorable for the low-wing model.

If the magnitude of the first effect is assumed to be almost independent of the vertical location of the wing, or at least to be less sensitive to wing location than the magnitude of the second effect, it is apparent that power will have a smaller adverse effect on the high-wing than on the low-wing model. This difference in effect of power will increase with lift coefficient.

As has been mentioned, one effect of power on effective dihedral is an increase in the lift over the part of the wing covered by the slipstream, which results in an unfavorable spanwise shift of the center of pressure when the airplane is yawed. In order to show the increase caused by power, the increments of lift coefficient between the windmilling and power-on conditions at the same angle of attack have been obtained from figure 11 and plotted in figure 12. As was expected, the curves of figure 12 showed the same trends as those of figure 9. Again an exception is noted in the curve for the low wing with double slotted flap, which is unreliable.

The foregoing discussion of the effects of power are summarized as follows:

(1) The application of power results in a decrease in effective dihedral.

(2) The adverse effect of power is greater when the wing is in the low location than when the wing is in the high location.

(3) The adverse effect of power generally increases with lift coefficient.

Effect of flap deflection.- The model with the double slotted flap was not tested at a lift coefficient low enough to permit the determination of the effect of this flap on effective dihedral; the curves of figure 10 therefore show the effect of only the single slotted flap.

Flap deflection appears to be unfavorable for both wing locations and for both power conditions.

The effect of flap deflection seems to be of the same order of magnitude for both the power-on and the windmilling conditions, and there seems to be no regular variation with lift coefficient. Flap deflection seems to have a slightly greater adverse effect on the low-wing than on the high-wing model. Tail-on tests of the same model (unpublished data) showed that the adverse effect of flap deflection was slightly greater for the high-wing than for the low-wing model.

The adverse effect of flap deflection on the effective dihedral of a swept-forward wing can be explained by considering separately the effect of yaw on the lift of each half of the wing. A swept-forward wing without flaps and with no dihedral is considered first. When the model is yawed, the trailing wing has a greater component of velocity normal to the quarter-chord line than the forward wing and thus has a greater lift. This difference in lift between the leading and the trailing wings results in an unfavorable rolling moment. By extending this reasoning to cover a range of angles of yaw, the slope of the curve of rolling-moment coefficient against angle of yaw is seen to be negative (negative effective dihedral). The opposite will be true, of course, for a swept-back wing. A more detailed analysis is given in reference 1. A wing with the flaps deflected is now considered. An analysis similar to the foregoing one can be applied to the additional lift caused by the flaps. In this case the velocities considered should be those normal to the hinge lines of the flaps. The analysis indicates that, if the flap hinge lines are swept forward (as on the

P-36A airplane), the flaps will give a negative increment of effective dihedral, regardless of wing sweep. This effect is illustrated in figure 10.

Since the increment in lift produced by deflecting the flaps can be considered constant throughout the range of lift coefficient, the increment in effective dihedral caused by flap deflection should also be constant. Although such is not quite the case in figure 10, there is no decided trend of the curves so that this reasoning seems to be valid and the variations of the curves from horizontal straight lines may be considered to be caused by other effects.

The foregoing discussion of the effects of deflecting the single slotted flap 30° is summarized as follows:

(1) The effect of flap deflection on effective dihedral is unfavorable for both wing locations and for both power conditions.

(2) This effect appears to be of the same order of magnitude for both the power-on and the windmilling conditions, for the limited range of thrust coefficients and lift coefficients investigated.

(3) Flap deflection appears to have a slightly greater adverse effect on the low-wing than on the high-wing model. Tail-on tests of the same model have showed a small opposite effect.

(4) There seems to be no definite variation of the effect of flap deflection with lift coefficient.

CONCLUSIONS

From tests in the Langley 7- by 10-foot tunnel of a modified $\frac{1}{5}$-scale model of the Curtiss P-36A airplane with the quarter-chord line of the wing swept forward 2.6° and the tail removed, the following conclusions were drawn regarding the effects of wing location, power, and flap deflection on effective dihedral:

Effect of wing location.-

(1) Changing the wing from the high to the low
location resulted in a decrease in effective dihedral.

(2) The difference in effective dihedral for the
high-wing and the low-wing models was greater for the
power-on condition than for the windmilling condition.

Effect of power.-

(1) The application of power resulted in a decrease
in effective dihedral.

(2) Power had a greater adverse effect for the
low-wing than for the high-wing model.

(3) The adverse effect of power generally increased
with lift coefficient.

Effect of flap deflection (full-span single slotted
flap only; flap hinge lines swept forward).-

(1) The effect of flap deflection on effective
dihedral was unfavorable for both wing locations and
for both the power conditions.

(2) The effect of flap deflection appeared to be
of the same order of magnitude for the power-on and the
windmilling conditions, for the limited range of thrust
coefficients and lift coefficients investigated.

(3) Flap deflection appeared to have a slightly
greater adverse effect on the low-wing than on the
high-wing model. Tail-on tests of the same model have
showed a small opposite effect.

(4) There seemed to be no definite variation of the
effect of flap deflection with lift coefficient. This
fact seems to substantiate a rough qualitative analysis,
which indicates that the effect of flap deflection should
not vary with lift coefficient.

Langley Memorial Aeronautical Laboratory
    National Advisory Committee for Aeronautics
        Langley Field, Va., January 2, 1945

REFERENCES

1. Betz, A.: Applied Airfoil Theory. Unsymmetrical and
      Non-Steady Types of Motion. Vol. IV of Aero-
      dynamic Theory, div. J, ch. IV, secs. 1-4,
      W. F. Durand, ed., Julius Springer (Berlin), 1935.

2. Pearson, Henry A., and Jones, Robert T.: Theoretical
      Stability and Control Characteristics of Wings
      with Various Amounts of Taper and Twist. NACA
      Rep. No. 635, 1938.

3. House, Rufus O., and Wallace, Arthur R.: Wind-Tunnel
      Investigation of Effect of Interference on Lateral-
      Stability Characteristics of Four NACA 23012 Wings,
      an Elliptical and a Circular Fuselage, and Vertical
      Fins. NACA Rep. No. 705, 1941.

4. Bamber, M. J., and House, R. O.: Wind-Tunnel Investi-
      gation of Effect of Yaw on Lateral-Stability
      Characteristics. II - Rectangular N.A.C.A. 23012
      Wing with a Circular Fuselage and a Fin. NACA
      TN No. 730, 1939.

5. Recant, Isidore G., and Wallace, Arthur R.: Wind-
      Tunnel Investigation of Effect of Yaw on Lateral-
      Stability Characteristics. III - Symmetrically
      Tapered Wing at Various Positions on Circular
      Fuselage with and without a Vertical Tail.
      NACA TN No. 825, 1941.

6. Recant, I. G., and Wallace, Arthur R.: Wind-Tunnel
      Investigation of Effect of Yaw on Lateral-
      Stability Characteristics. IV - Symmetrically
      Tapered Wing with a Circular Fuselage Having a
      Wedge-Shaped Rear and a Vertical Tail. NACA ARR,
      March 1942.

7. Wallace, Arthur R., and Turner, Thomas R.: Wind-
      Tunnel Investigation of Effect of Yaw on Lateral-
      Stability Characteristics. V - Symmetrically
      Tapered Wing with a Circular Fuselage Having a
      Horizontal and a Vertical Tail. NACA ARR
      No. 3F23, 1943.

WTRL-459

8. Multhopp, H.: Aerodynamics of the Fuselage. NACA TM
      No. 1036, 1942.

9. Harris, Thomas A.: The 7 by 10 Foot Wind Tunnel of
      the National Advisory Committee for Aeronautics.
      NACA Rep. No. 412, 1931.

10. Wenzinger, Carl J., and Harris, Thomas A.: Wind-
      Tunnel Investigation of an N.A.C.A. 23012 Airfoil
      with Various Arrangements of Slotted Flaps.
      NACA Rep. No. 664, 1939.

11. Harris, Thomas A., and Recant, Isidore G.: Wind-
      Tunnel Investigation of NACA 23012, 23021, and
      23030 Airfoils Equipped with 40-Percent-Chord
      Double Slotted Flaps. NACA Rep. No. 723, 1941.

12. Ribner, Herbert S.: Proposal for a Propeller
      Side-Force Factor. NACA RB No. 3L02, 1943.

Fig. 1
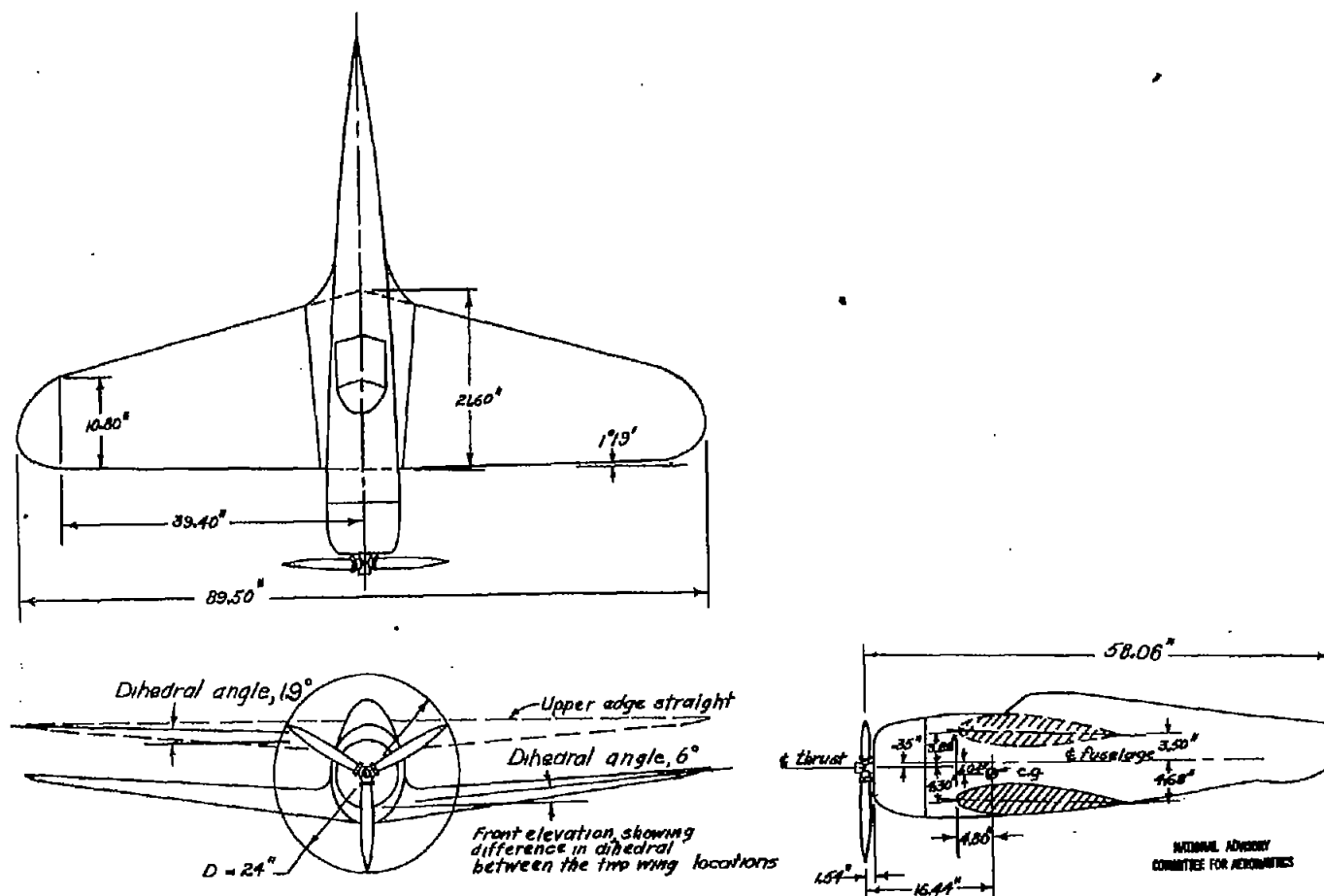
Figure 1. – Modified $\frac{1}{5}$-scale model of Curtiss P-36A airplane with tail removed. Neither single slotted nor double slotted flaps are shown. See figure 2 for flap details.

Fig. 2

3.80"

Flaps extend in to this line for high wing

41.80"

Lip

Nose

Lip

Nose

21.60'

10.80"

1°19'

39.40"

44.75"

(a) Plan form of wing; $\frac{1}{5}$ scale.

.28c

.18c

.25c

.40c

Flaps retracted

Single slotted flaps, $\delta_f = 30°$

Double slotted flaps;
$\delta_{f_1} = \delta_{f_2} = 30°$

NATIONAL ADVISORY
COMMITTEE FOR AERONAUTICS

(b) Typical section, showing
various flap arrangements;
no scale.
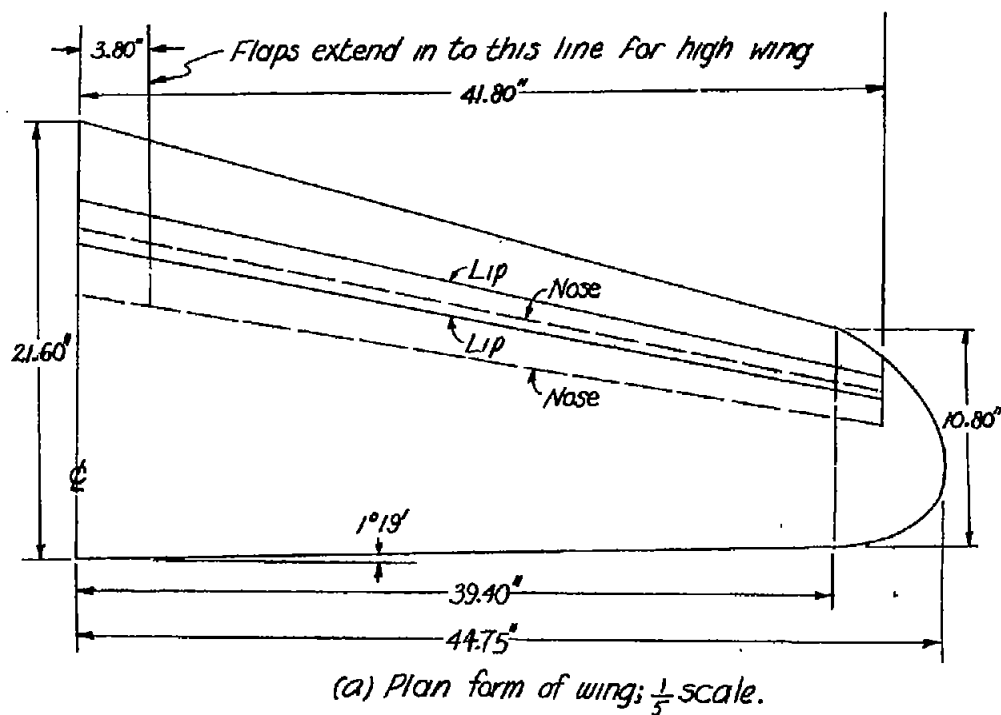
Figure 2.- Flap details of the modified $\frac{1}{5}$-scale
model of the Curtiss P-36A airplane.

Fig. 3
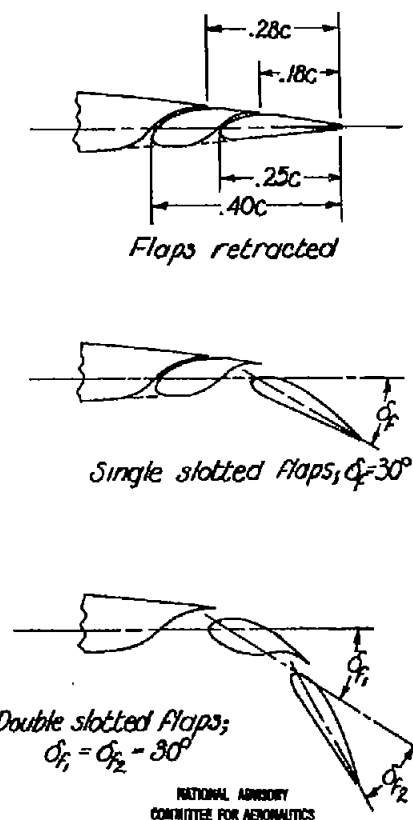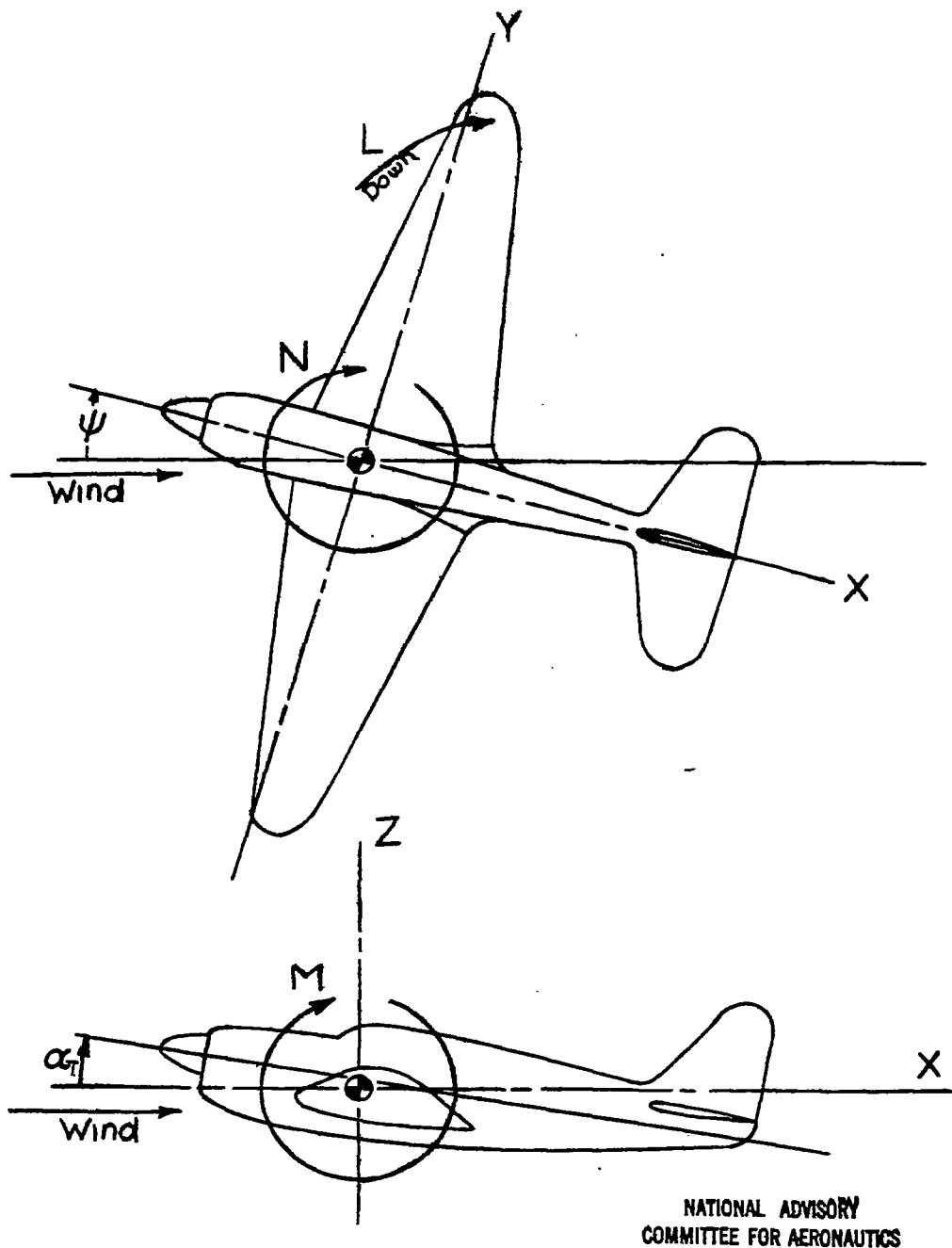
Figure 3.- Notation of axis system
used. Arrows indicate positive directions.

NATIONAL ADVISORY
COMMITTEE FOR AERONAUTICS

Fig. 4   NACA TN No. 1061
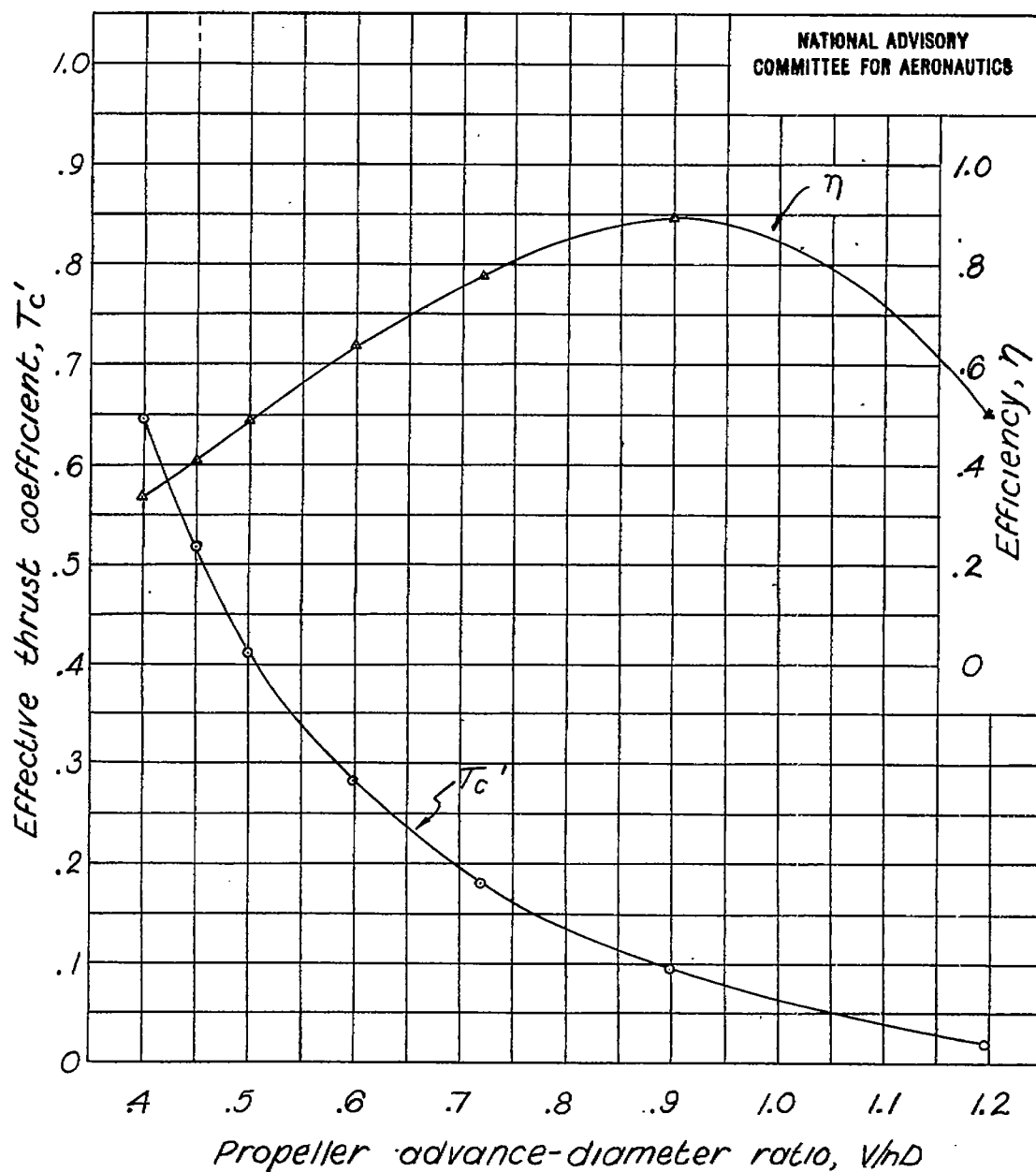
Figure 4.- Effective thrust coefficient and efficiency as functions of propeller advance-diameter ratio for the modified ½-scale model of the Curtiss P-36 A airplane. D=2.0 feet; β=25°.
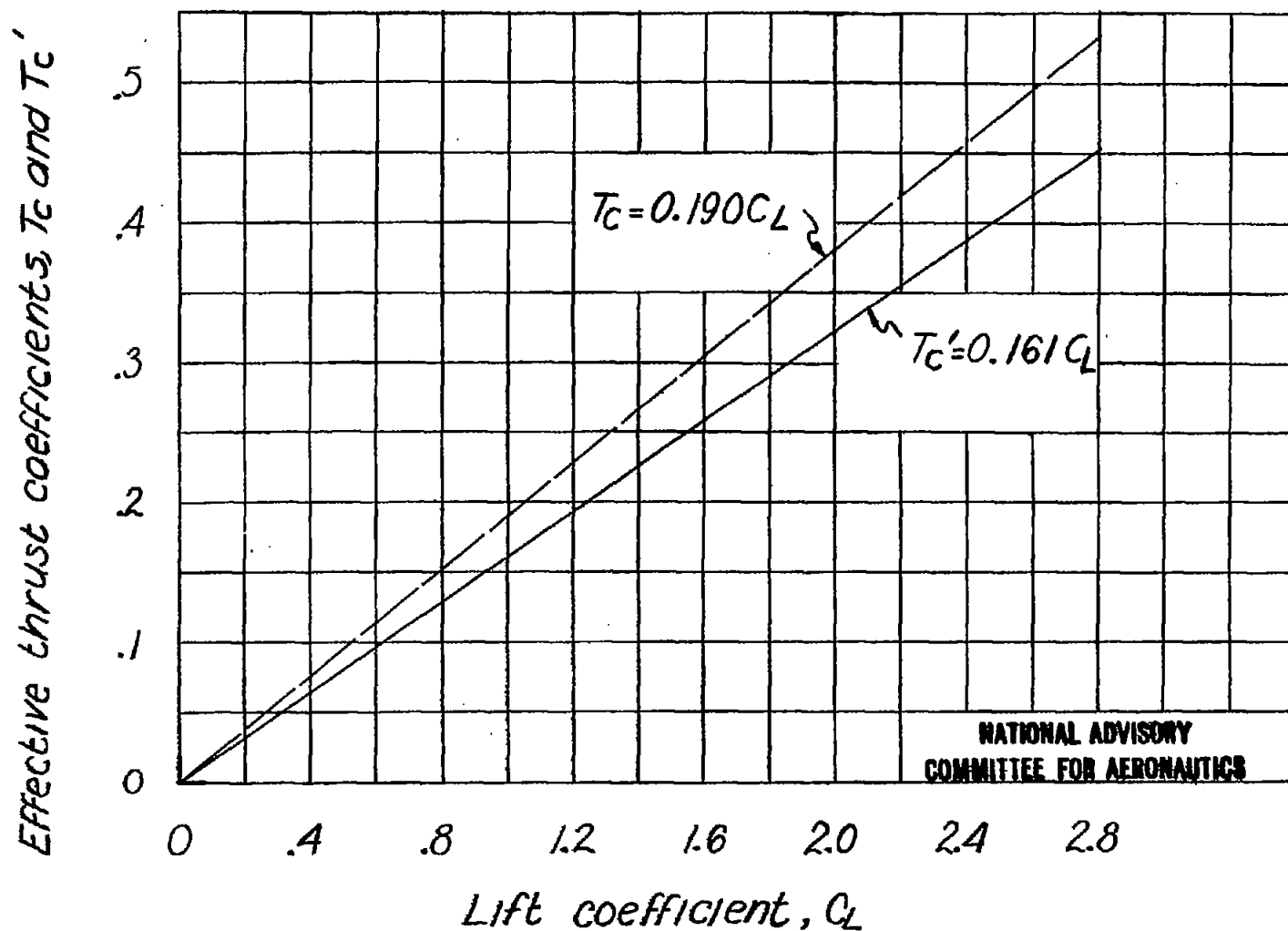
Figure 5.- Variation of effective thrust coefficients with lift coefficient.

$$T_C = 0.190 C_L$$

$$T_C' = 0.161 C_L$$

NATIONAL ADVISORY
COMMITTEE FOR AERONAUTICS

Fig. 5

Fig. 6   NACA TN No. 1061
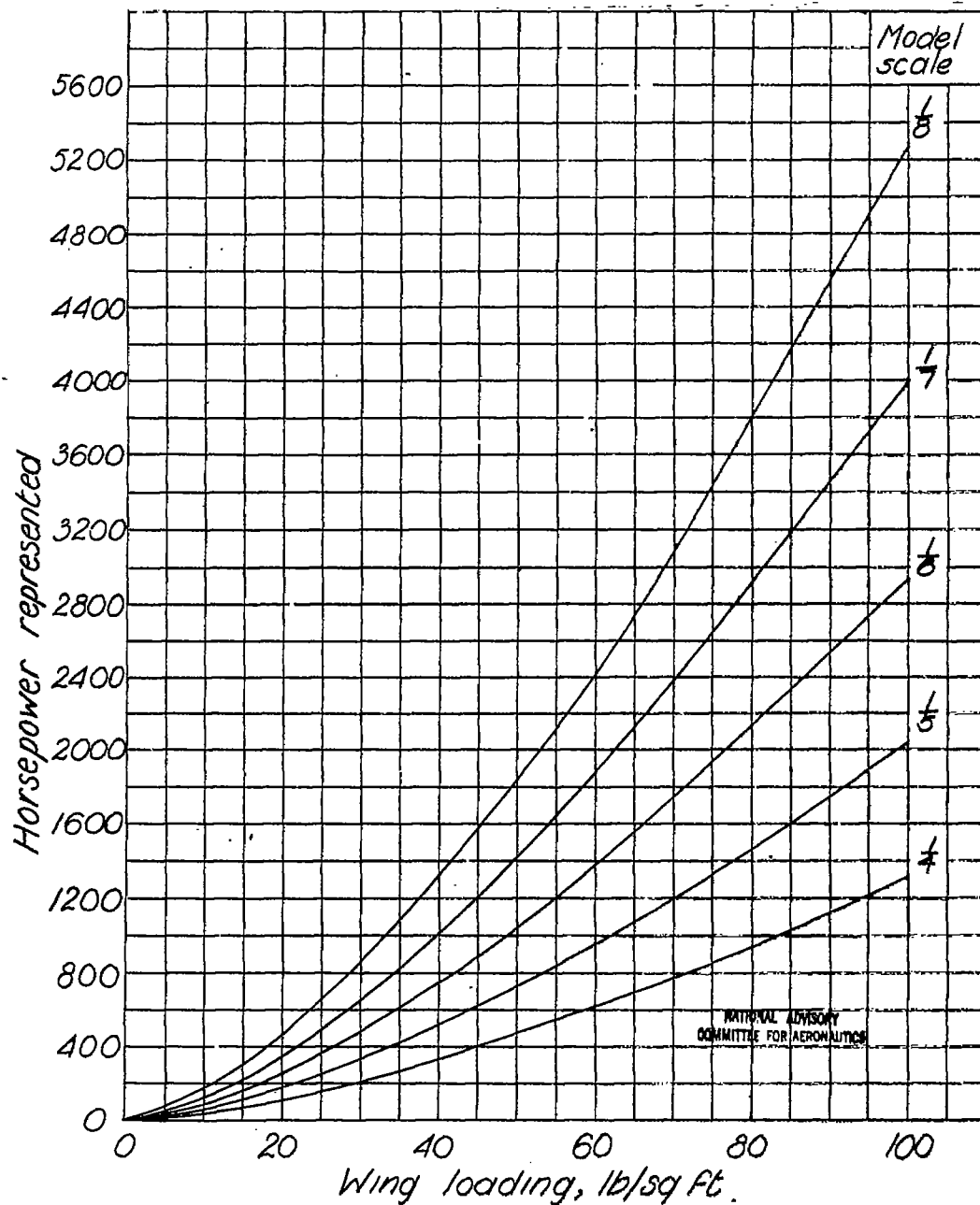
Figure 6.- Variation of approximate horsepower
represented with airplane wing loading
for various model scales.
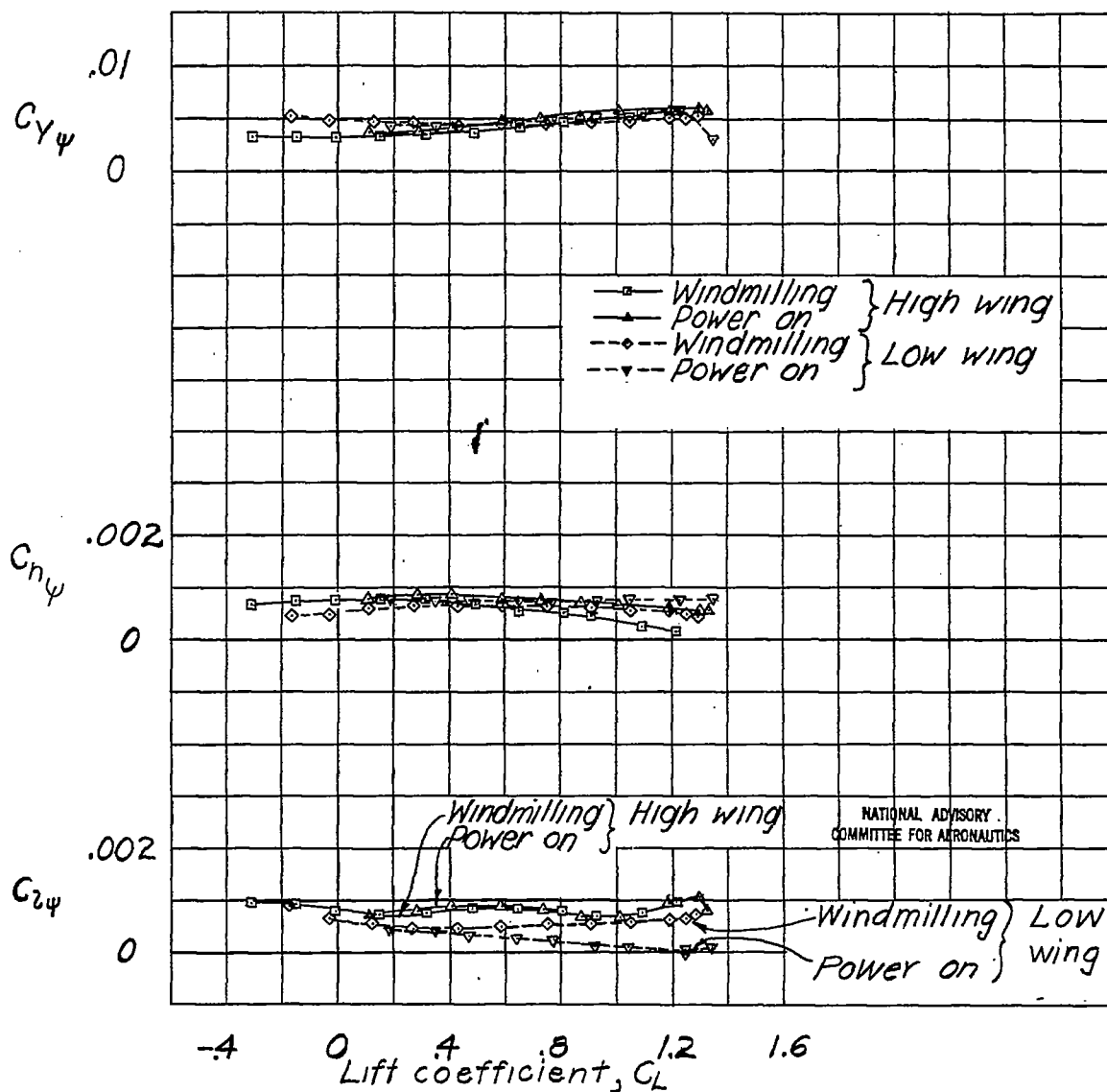
(a) Flaps retracted.

Figure 7.-Effect of wing location and power on the parameters C_{l_ψ}, C_{n_ψ}, and C_{Y_ψ}. Modified ⅓-scale model of the Curtiss P-36A airplane; tail removed.
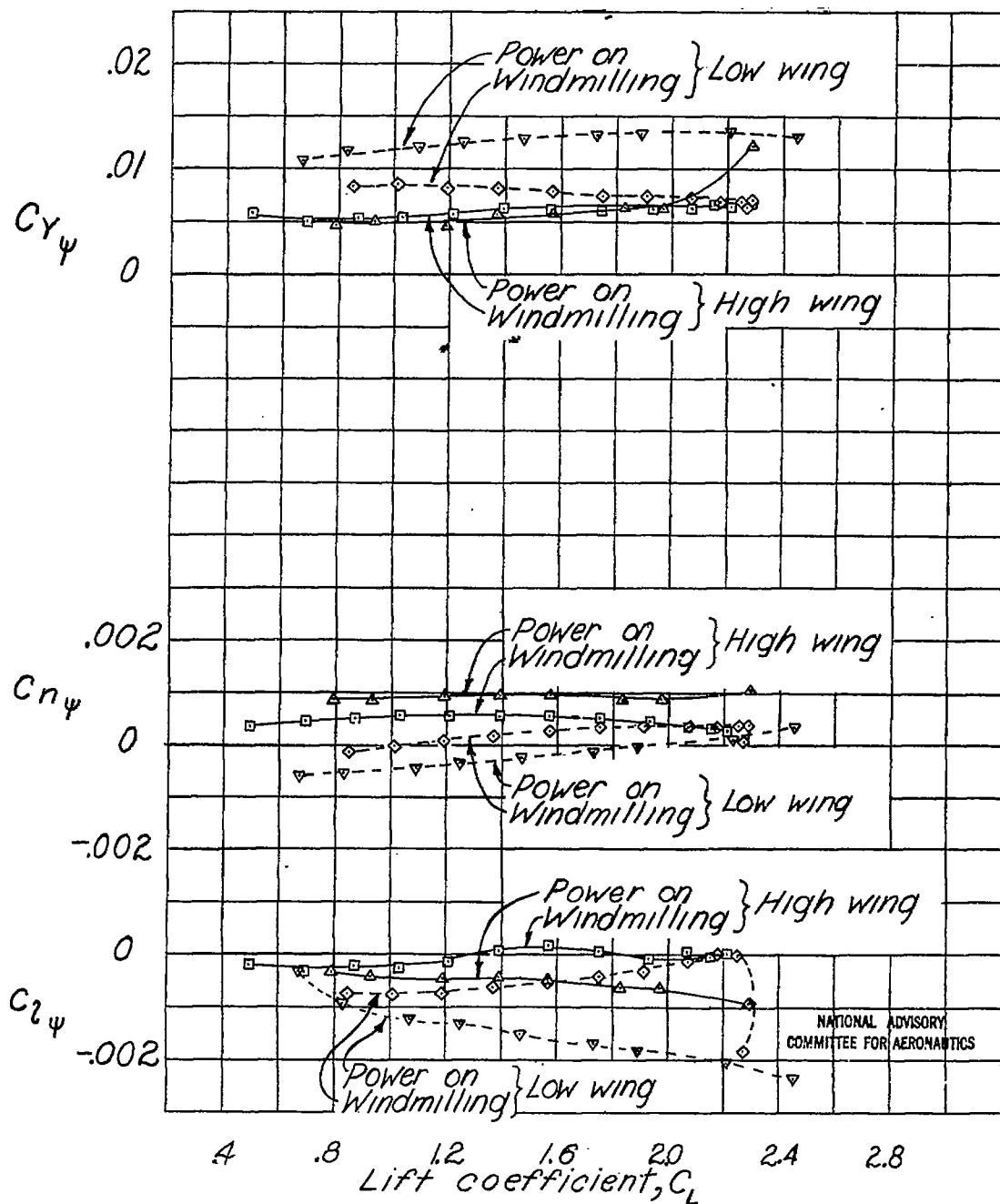
(b) Full-span single slotted flaps; $\delta_f = 30°$.

Figure 7.—Continued.
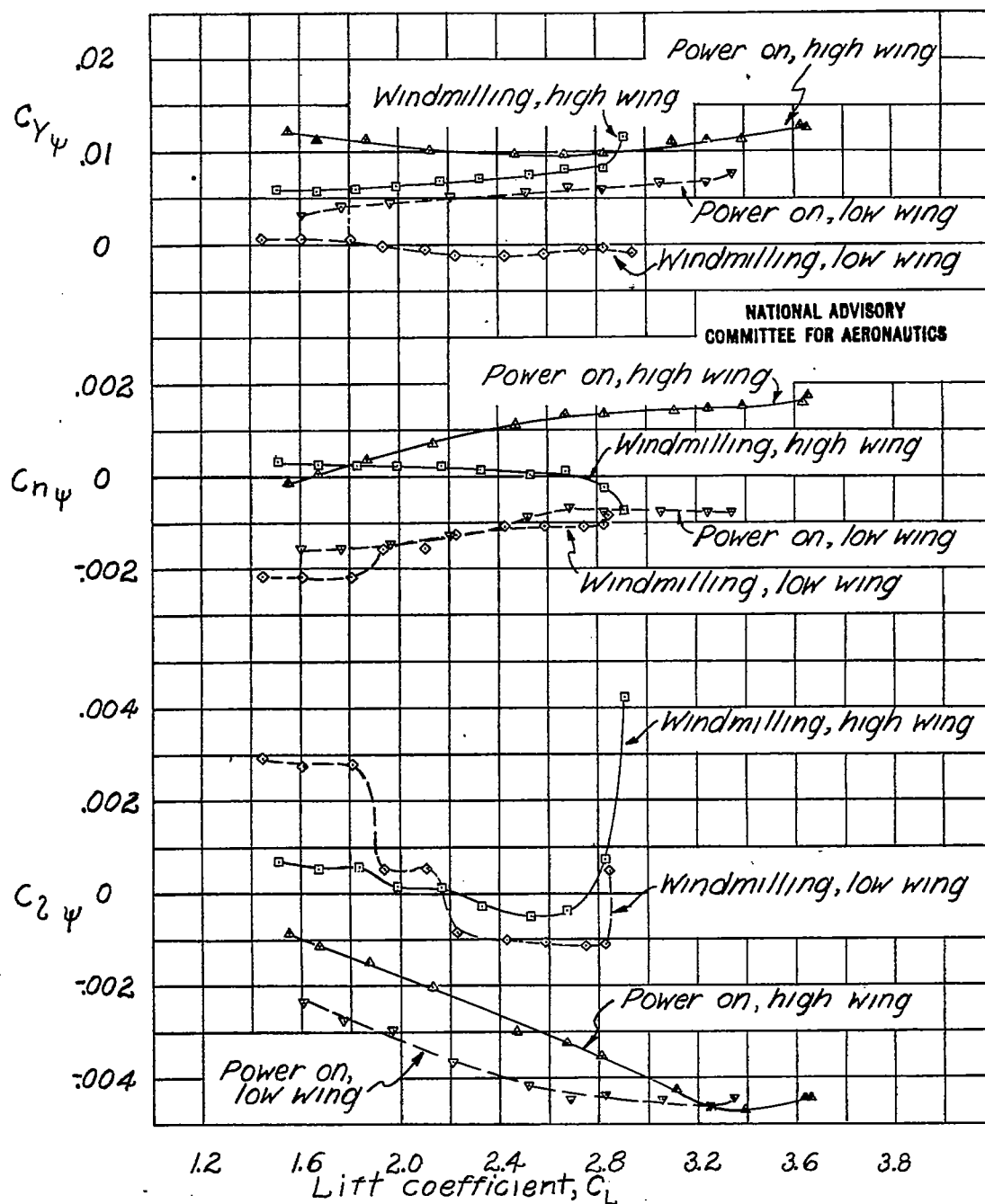
(c) Full-span double slotted flaps; $\delta_{F_1} = \delta_{F_2} = 30°$.

Figure 7.—Concluded.

Fig. 8   NACA TN No. 1061
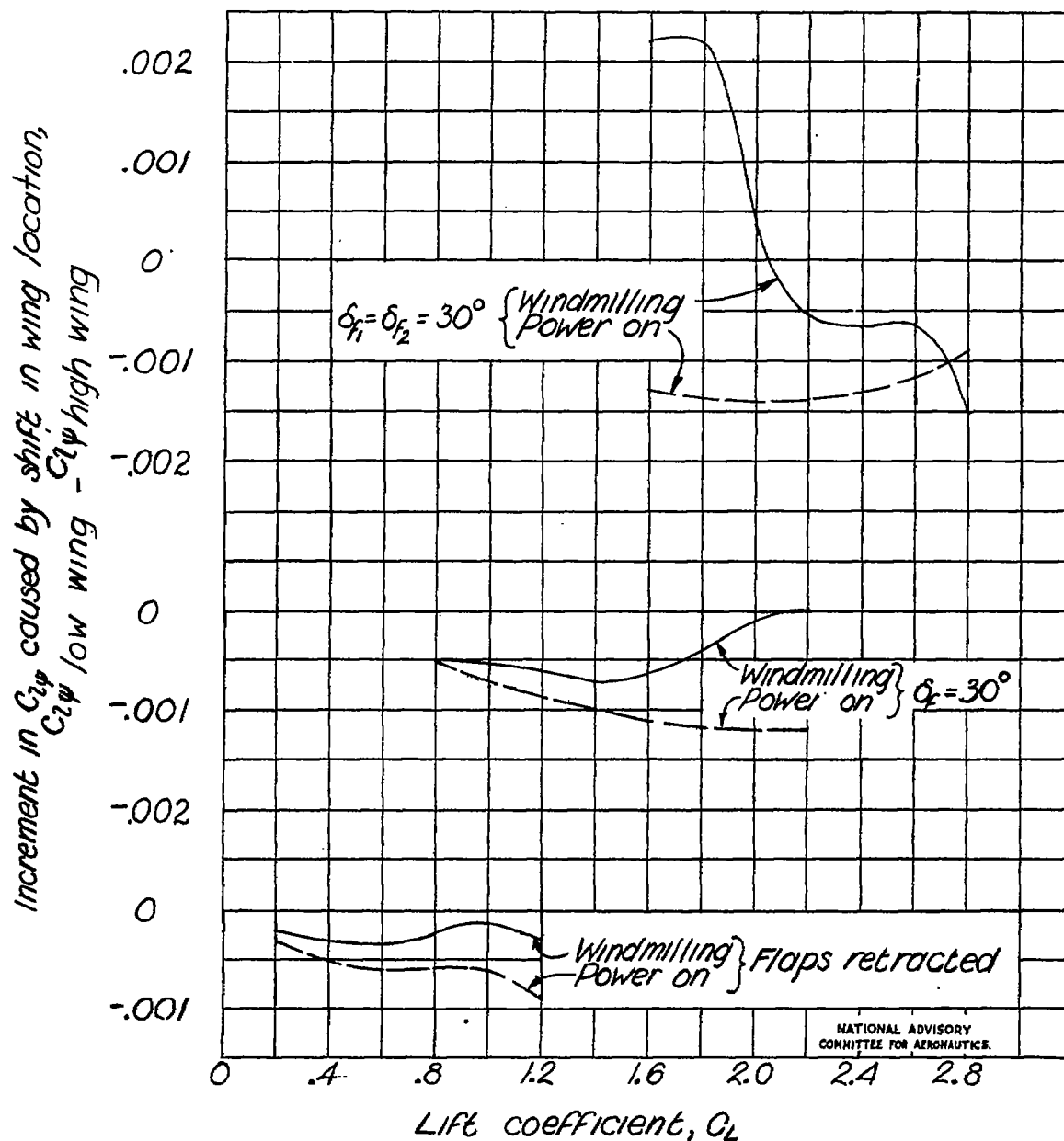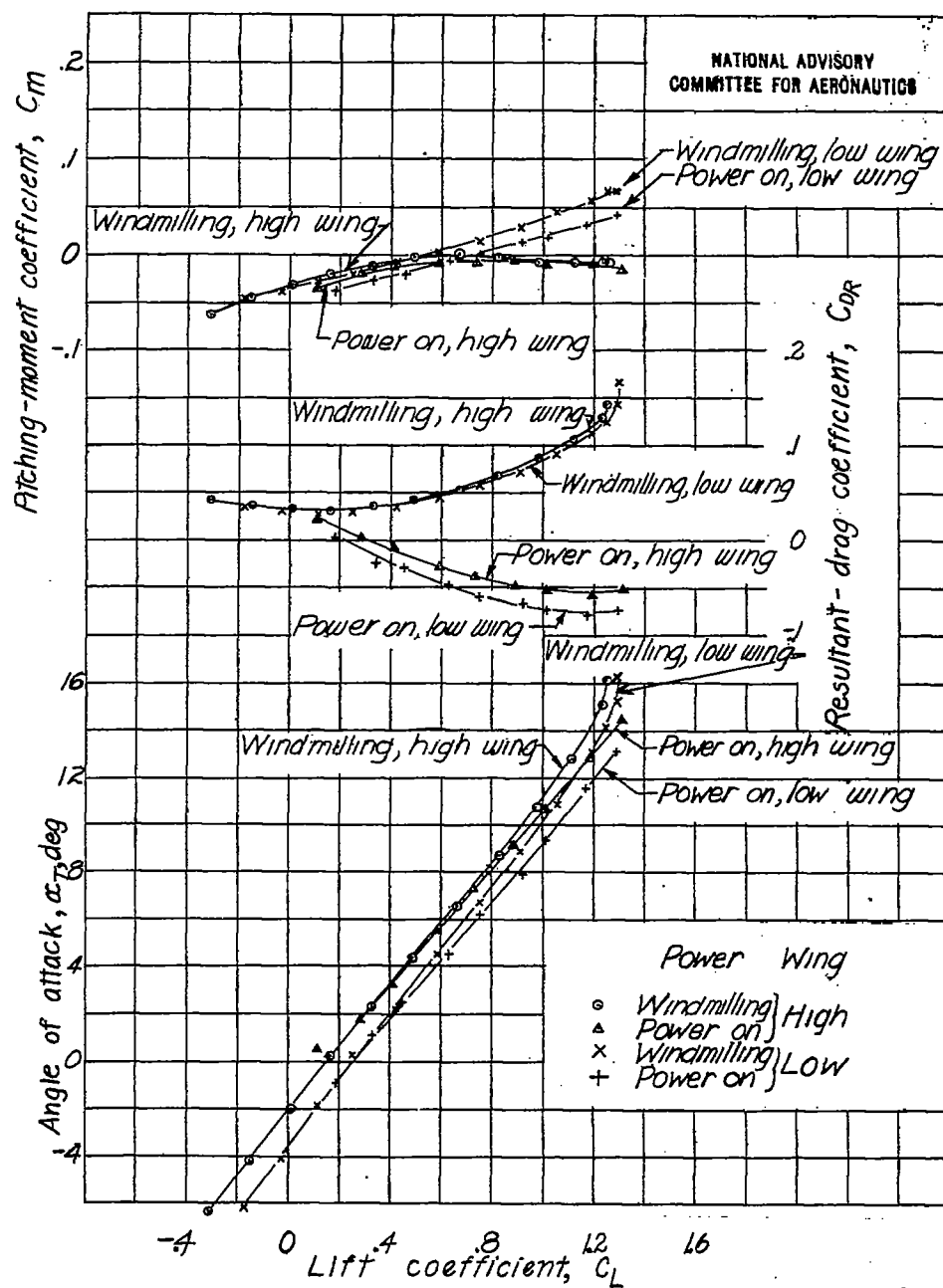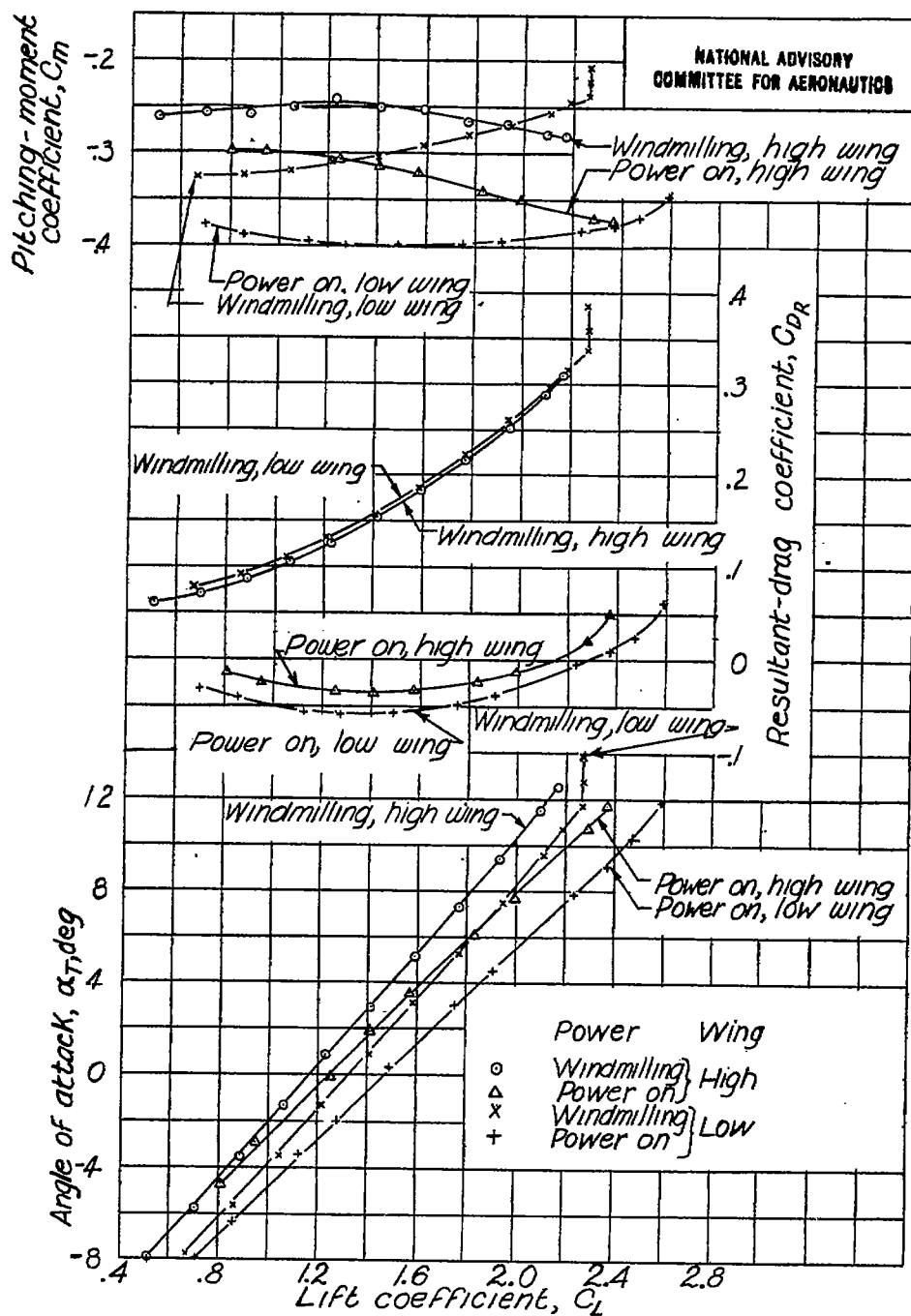

Figure 8 .- Effect of wing location on $C_{l\psi}$. Modified $\frac{1}{5}$ - scale model of the Curtiss P-36A airplane; tail removed.
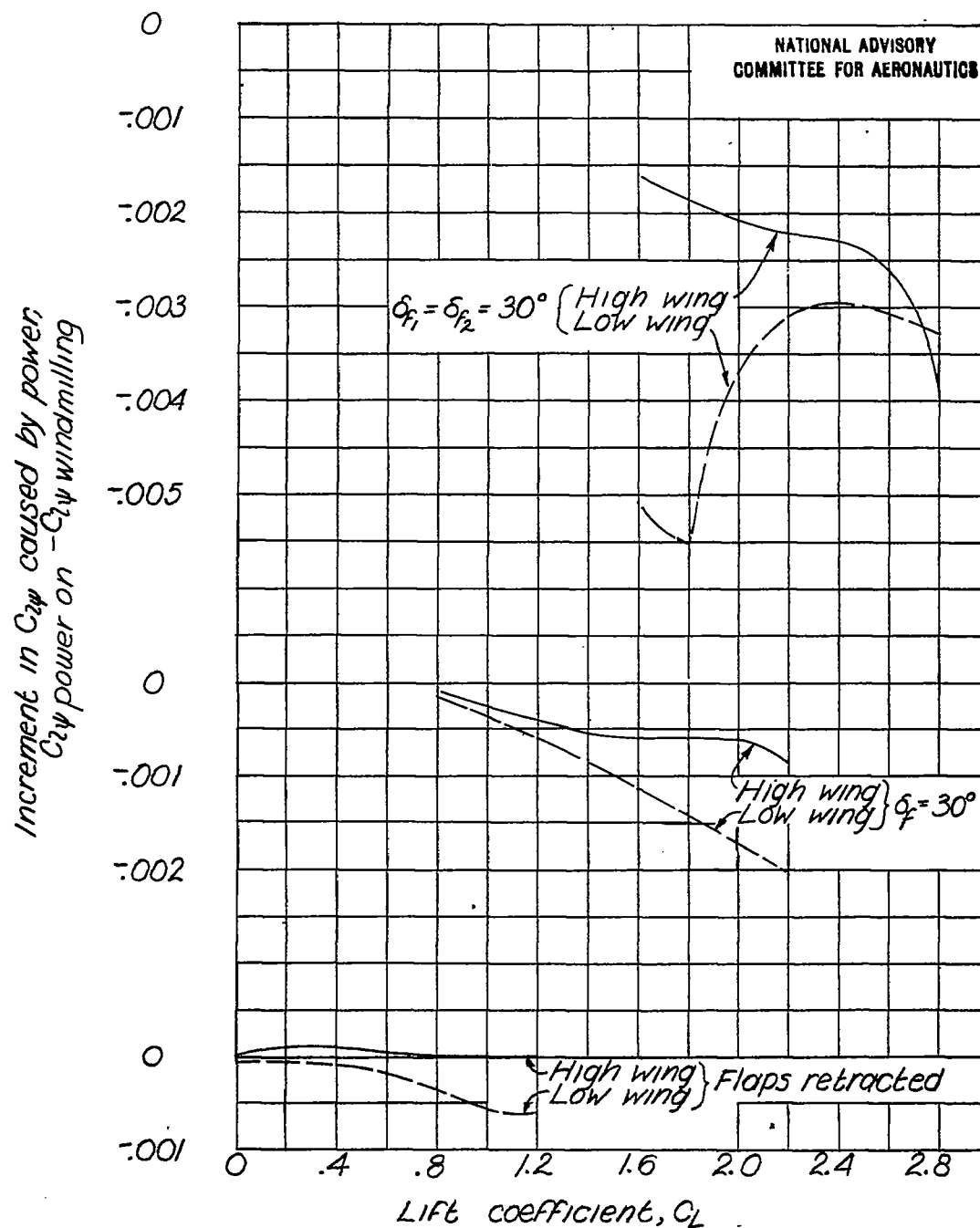
Figure 9.— Effect of power on $C_{l\psi}$. Modified $\frac{1}{5}$ - scale model of the Curtiss P-36A airplane; tail removed.

Fig. 10
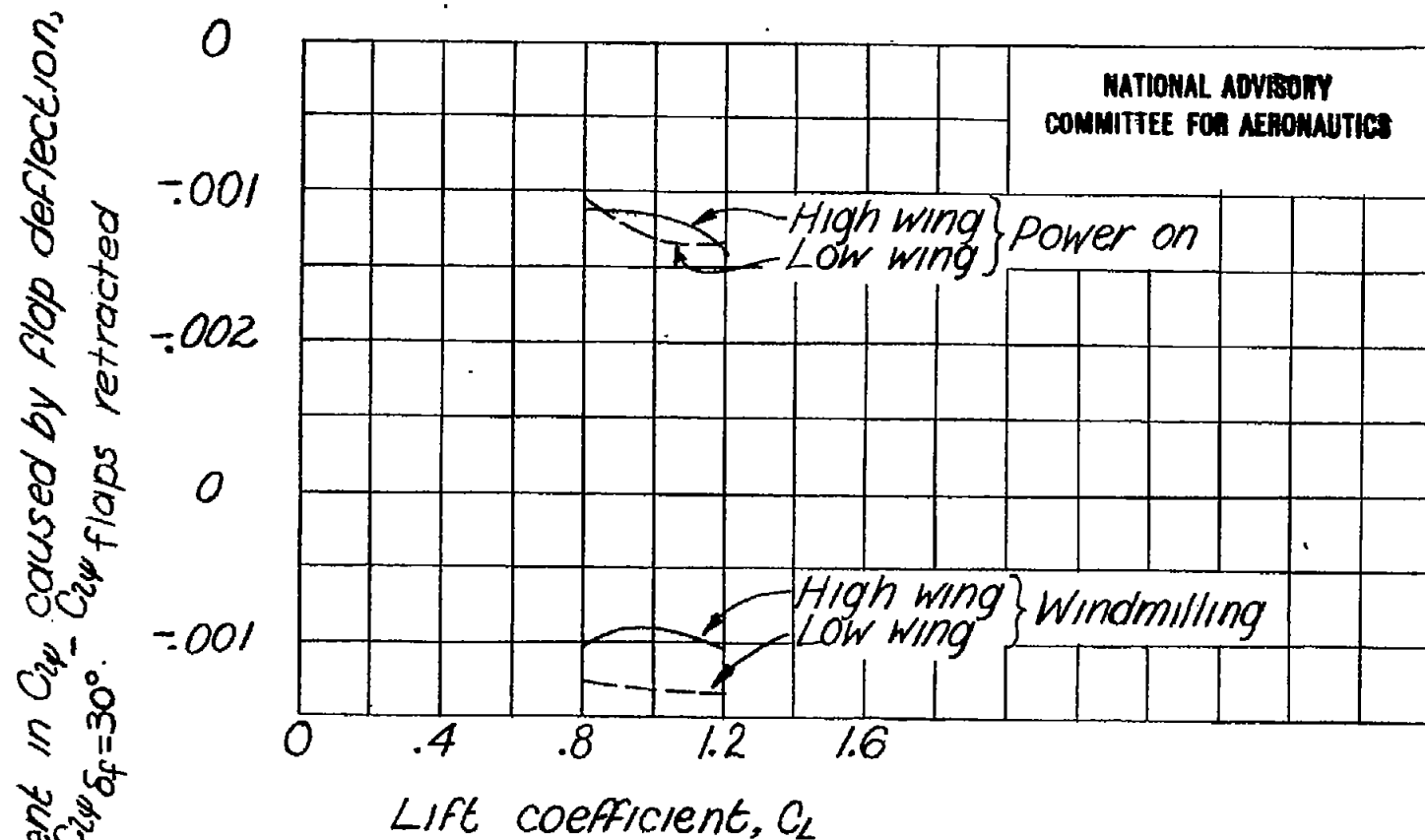
Figure 10.- Effect of flap deflection on $C_{l\psi}$. Modified $\frac{1}{5}$-scale model of the Curtiss P-36 A airplane, tail removed; full-span single slotted flap.
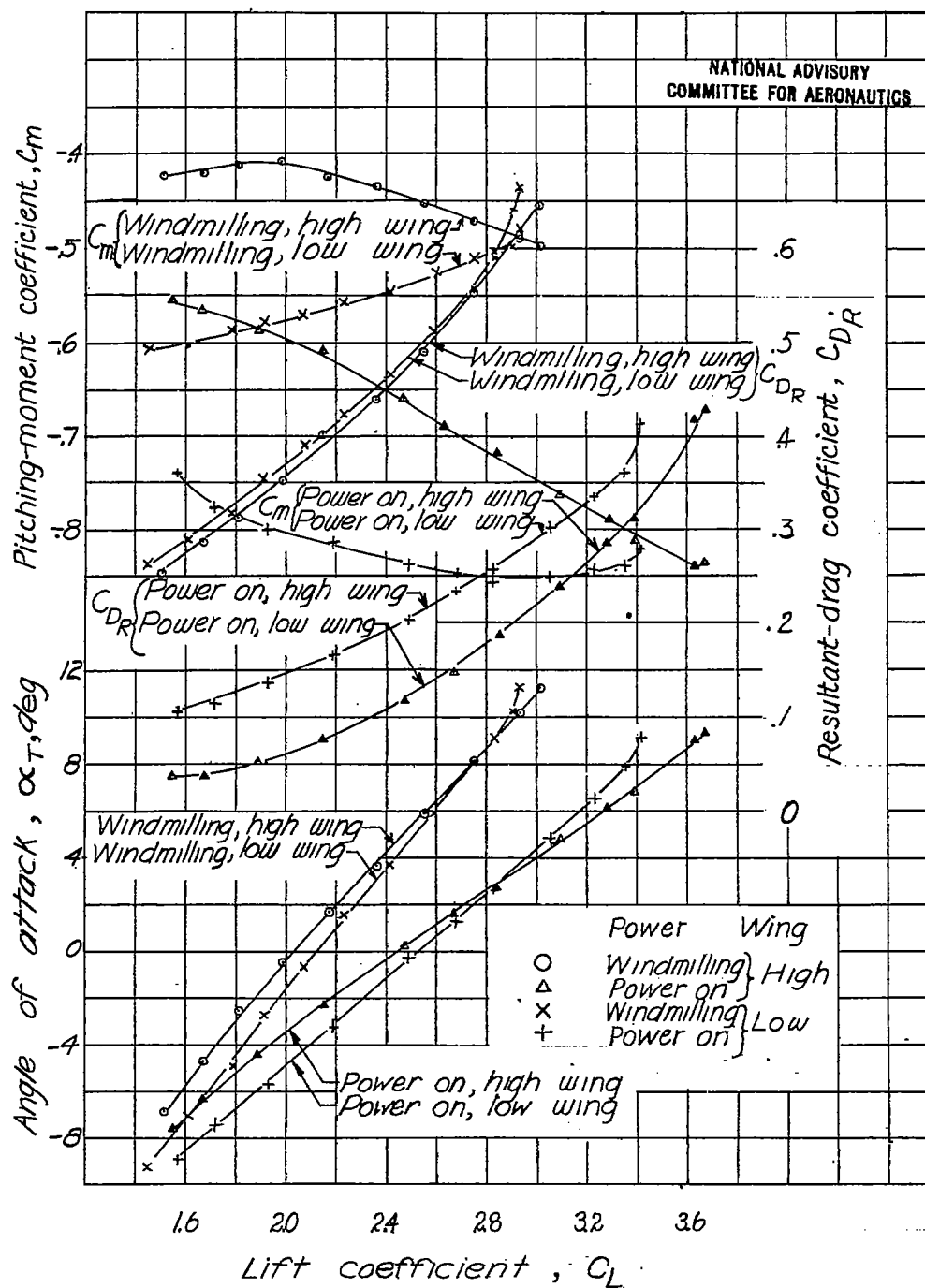
(a) Flaps retracted.

Figure 11.- Effect of wing location and power on the aerodynamic characteristics in pitch of a modified ⅕-scale model of the Curtiss P-36A airplane; tail removed; ψ=0°.

(b) Full-span single slotted flaps; $\delta_f = 30°$.

Figure 11.— Continued.

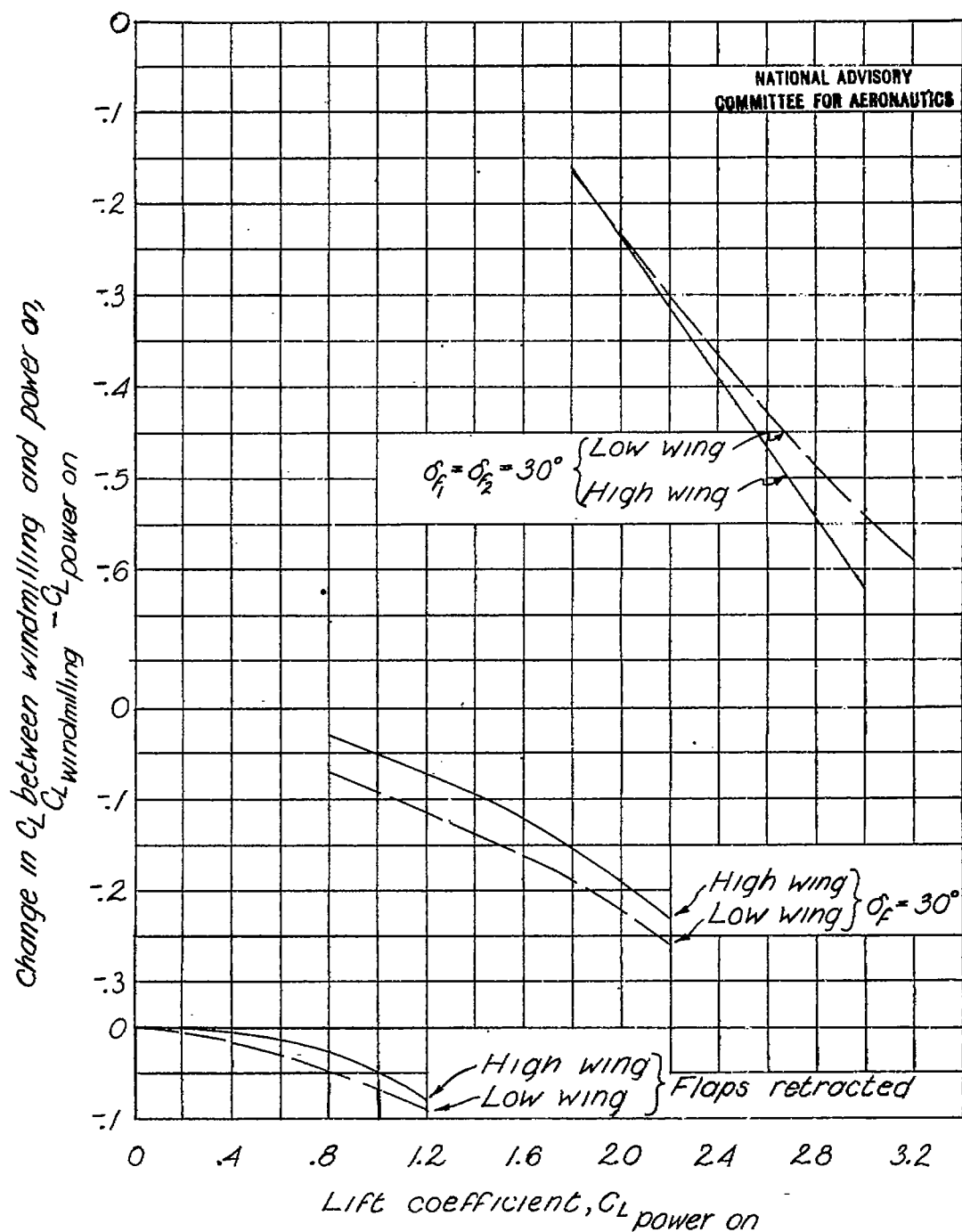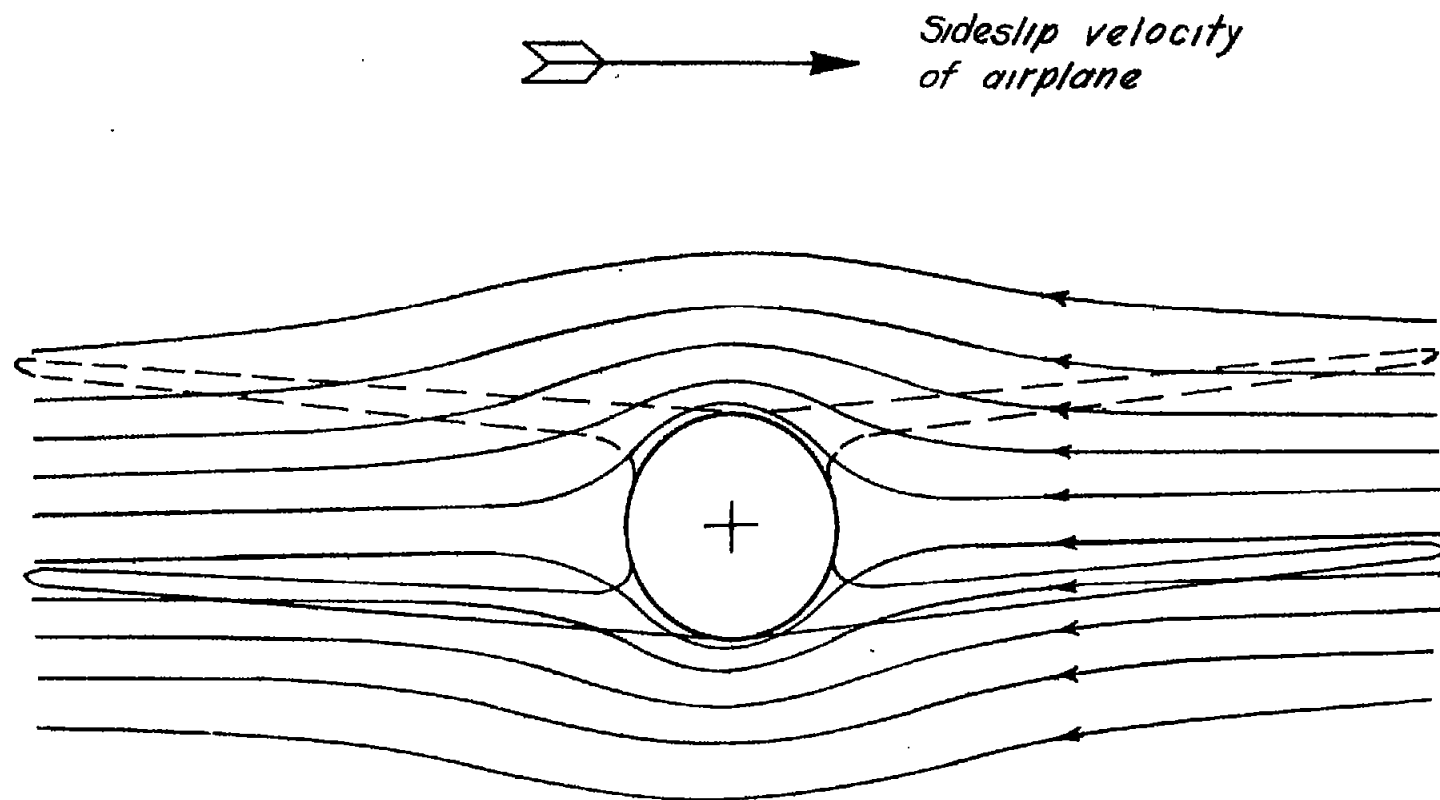(c) Full-span double slotted flaps; $\delta_{F_1}=\delta_{F_2}=30°$.

Figure 11.- Concluded.

Fig. 12   NACA TN No. 1061

Figure 12.—Effect of power on lift coefficient. Modified $\frac{1}{5}$-scale model of the Curtiss P-36A airplane; tail removed.

Sideslip velocity
of airplane

National Advisory
Committee for Aeronautics

Figure 13.- Transverse flow caused by sideslip.

Fig. 13